Progress In Electromagnetics Research, Vol. 141, 769–784, 2013

EXPERIMENTAL STUDY OF EFFICIENT WIRELESS POWER TRANSFER SYSTEM INTEGRATING WITH HIGHLY SUB-WAVELENGTH METAMATERIALS

Yingchun Fan, Long Li*, Shixing Yu, Chen Zhu, and Changhong Liang

School of Electronic Engineering, Xidian University, Xi'an, Shanxi 710071, China

Abstract—In this paper, an efficient wireless power transfer (WPT) system integrating with highly sub-wavelength metamaterials is proposed. The negative refractive index (NRI) and negative permeability (MNG) metamaterials for operation at radio frequencies are designed and applied to WPT system for improvement of power transfer efficiency. A dual-layer design which consists of a planar spiral on one side and a meander line touching with narrow metallic strips on the other side produces the properties of effective negative permittivity and permeability simultaneously, i.e., negative refractive index. In addition, the structure of double spirals produces a negative permeability. The cell size of the NRI and MNG metamaterials is about 253 times smaller than the operation wavelength. By integrating one, two, three or four metamaterial slabs between the two coupling copper rings, the transfer efficiency is improved significantly. The measured results show that the contribution of high transfer efficiency is due to the property of negative permeability which can make the WPT system work in the mechanism of magnetic resonance.

1. INTRODUCTION

Wireless power transfer (WPT) technology was first proposed by Nikola Tesla at the turn of the 20th century [1]. Recently, a mid-range non-radiant wireless power transfer technology was proposed by Kurs et al. [2]. So far, there have been mainly three methods for WPT, namely radiant WPT technology, inductive coupling WPT technology and resonant coupling WPT technology. Radiant WPT

Received 17 June 2013, Accepted 30 July 2013, Scheduled 16 August 2013
* Corresponding author: Long Li (lilong@mail.xidian.edu.cn).

technology relies on the transfer of the electromagnetic waves, which could be widely applied in space transfer and satellite solar power station. Inductive coupling WPT is also an efficient technique brought into practice, but it can only be used as a short-distance WPT [3].

Resonant coupling WPT is based on the magnetic resonance theory and is a non-radiant WPT method which relies mainly on near field resonant coupling. The transfer distance is generally several times of the size of the transfer device [2]. The schematic circuit of magnetic resonant coupling WPT is shown in Fig. 1 [4]. The circuit parameters of the source coil are L_S and C_S, and those of the device coil are L_D and C_D. R_S and R_D are the resistances of the source and device coils, respectively. Generally, the resonant frequencies of the source and device coils are adjusted to be the same. And the operating frequency is also adjusted to be the same as the resonant frequencies of the source and device coil, i.e., $f = 1/2\pi\sqrt{L_S C_S} = 1/2\pi\sqrt{L_D C_D}$. The transfer distance and transfer efficiency are compromised in this mechanism.

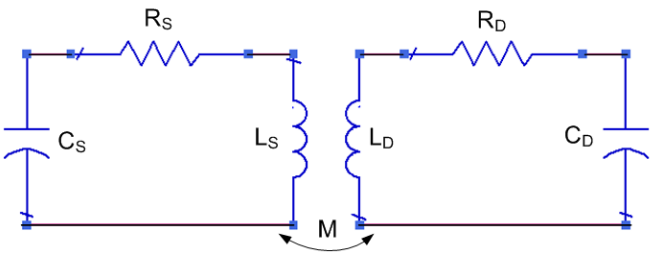

Figure 1. Equivalent schematic circuit of the resonant coupling WPT.

An efficient and miniaturized WPT system will enable advances in such areas as micro-robotics, medical treatment, mining and portable electronic devices [4]. But each of the above three methods has its limit in practical use, either the efficiency or the size of the transfer system. Recently, metamaterials with a μ-response have been shown to enhance WPT efficiency [5, 6]. In 2011, Urzhumov and Smith proposed a power relay system based on a near field metamaterial super lens, and presented a thorough analysis of this system. They showed that even with a realistic magnetic loss tangent of order of 0.1, the efficiency of power transfer with the slab can be an order of magnitude greater than free-space efficiency when the load exceeds a certain threshold value [7]. At present, the unit size of metamaterials is approximate 1/10 of the resonant wavelength, and the large size at low frequencies causes the metamaterials unable to use in practice. So the key problems of the WPT system with metamaterials focus mainly on the realization of metamaterials working at radio frequencies in small size and loss, and the combination of metamaterial slabs and the WPT system. The influence of the properties of metamaterials on the transfer efficiency must be taken into consideration.

This paper first introduces a kind of highly sub-wavelength negative refractive index (NRI) metamaterials which can work at radio frequencies (HF band) [8]. The NRI metamaterials have a dual-layer design consisting of planar spirals and meandering lines with covering metallic strips which makes the model satisfy the Lorentz-Drude model [8–12]. This kind of metamaterials may be used to improve the transfer efficiency of the wireless power transfer system. Without the covering strips, the metamaterials will not have the property of negative refractive index but have the property of negative permeability (MNG) while they can also be used to improve the WPT efficiency. Therefore, a comparison is made between the WPT system with NRI metamaterials and that with MNG metamaterials. Another kind of metamaterials with the property of negative permeability (MNG), which follows the idea of [12], is also proposed and will also be utilized to improve the WPT system in this paper. Experimental results show that the enhancement in efficiency is caused by the property of negative permeability. On condition that the system is well matched, the efficiency can be denoted by the square of S_{21} approximately. So we will compare S_{21} of different systems by making use of the full-wave, finite-element based simulation software HFSS and simulator ADS. The measured results show that the miniaturized WPT system with the proposed metamaterials can work perfectly in improving the transfer efficiency and transfer distance.

2. ANALYSIS OF HIGHLY SUB-WAVELENGTH NRI METAMATERIALS

We first propose a kind of highly sub-wavelength negative refractive index metamaterials [8], which has the advantages of small size and operation at radio frequencies (RFs) and can be used for WPT system. This kind of metamaterial structure consists of a dual-layer design by etching both sides of a substrate slab. One side of the slab is etched to be square spirals linking with a circle patch, and the other side is etched to be meandering lines, as shown in Fig. 2. Two narrow metallic strips are coated above and under the narrow side of the slab, and the meandering lines should be extended to touch the two strips. The metamaterials can have effective negative permeability and permittivity at low frequencies, simultaneously, i.e., negative refractive index, which obey the Lorentz-Drude model [8–12]. It is worth pointing

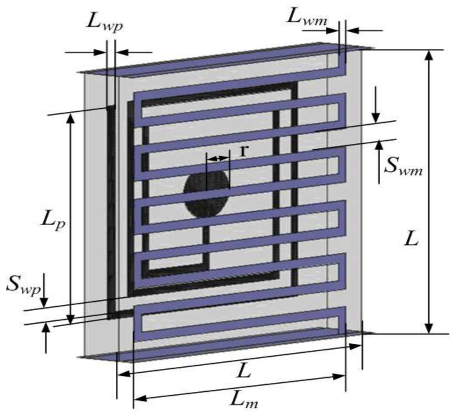

Figure 2. Solid view of the proposed NRI metamaterial geometry.

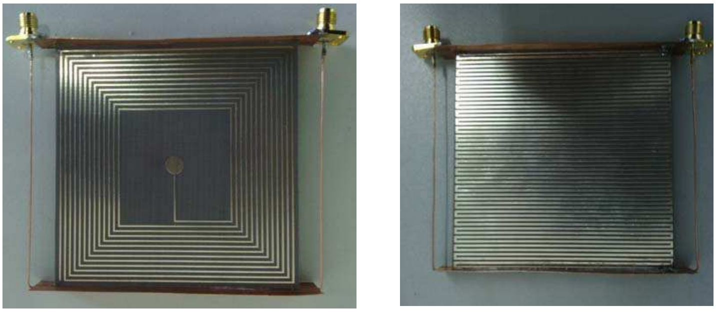

(a) (b)

Figure 3. (a) Top view photograph of the fabricated NRI metamaterials, (b) back view photograph of the fabricated NRI metamaterials.

out that without the two coated strips, the property of negative refractive index cannot be achieved, but the property of negative permeability in relative lower frequency can be obtained because of the mutual coupling of the spirals and meandering lines. The parameters of the structure are listed in Table 1. The substrate thickness is 1 mm, and the relative permittivity is 2.6 with loss tangent of 0.015. The top and back view photographs of the fabricated NRI metamaterials are shown in Figs. 3(a) and (b), respectively.

For the sake of clarity and completeness, here we give the simulation and measurement results of the retrieved effective parameters of relative permittivity ε_r, relative permeability μ_r, and

Table 1. Parameters of NRI metamaterials (UNIT: mm).

L	r	L_p	L_{wp}
78	3	75	0.6
S_{wp}	L_m	L_{wm}	S_{wm}
1	76.8	0.9	0.6

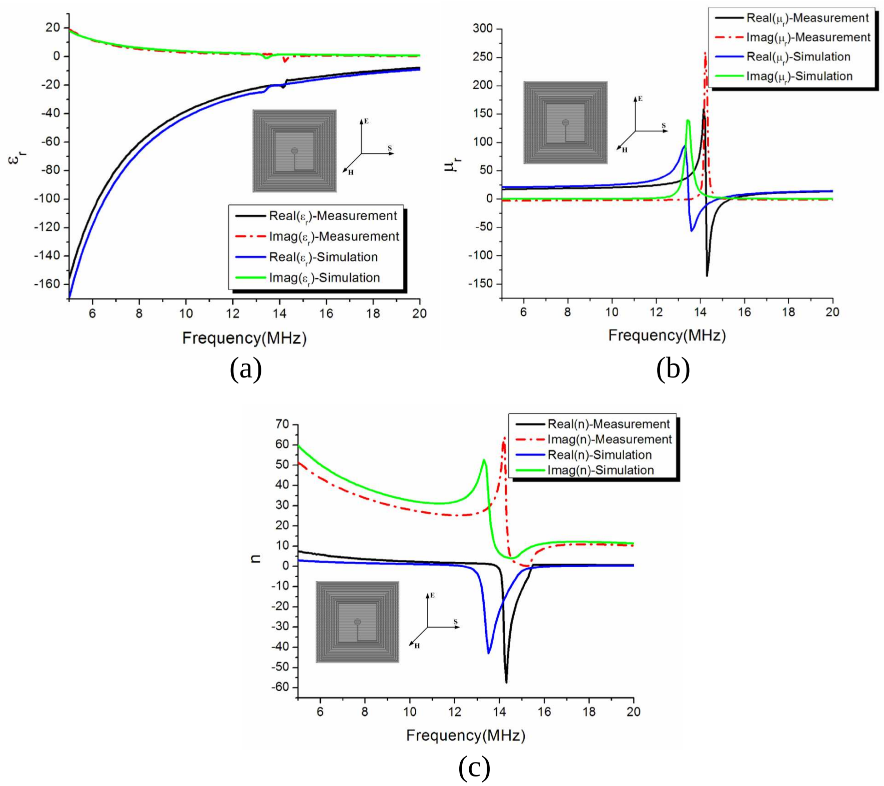

Figure 4. Simulated and measured retrieved results of the NRI metamaterials. (a) Effective permittivity, (b) effective permeability, and (c) effective refractive index.

refractive index n again, as shown in Fig. 4 [8, 13]. The periodicity of the proposed metamaterials is 78 mm when computing the effective material properties. It is the width of the metamaterial cell through which the electromagnetic wave passes. The measurement results agree well with the simulation ones although there is a little frequency shift caused by the fabrication error of the permittivity of the practical substrate in the experiment. The detailed analysis can be found in [8]. Compared with the metamaterials proposed by Chen et al. [12], our proposed metamaterials have not only negative permeability but also negative permittivity. Besides, it has the advantage of large sub-wavelength, and the ratio of the resonant wavelength to its unit size (λ_0/L) is greater than 253.

3. WPT SYSTEMS WITH METAMATERIALS

In this paper, an improved WPT system which combines the coupling rings with the highly sub-wavelength metamaterial slabs is proposed and analyzed. If placing one or more metamaterial slabs between the two coupling rings, we can see that the efficiency of power transfer will be increased significantly. The reason for the enhancement of transfer efficiency is that the coupling mechanism may be changed to resonant coupling when one or more NRI/MNG metamaterial slabs are put between the two coupling rings. And the efficiency of resonant coupling is great in mid-range. So the transfer distance and transfer efficiency are considerably improved upon putting one or more metamaterial slabs between the two rings.

3.1. WPT System with One Metamaterial Slab

Case 1. WPT System with One NRI Metamaterial Slab

The WPT system model with one NRI metamaterial slab is shown in Fig. 5. Only one cell is put between the two coupling rings. A photograph of the measured system is shown in Fig. 6. R is the outer radius of the copper ring, r_{in} the diameter of the copper ring,

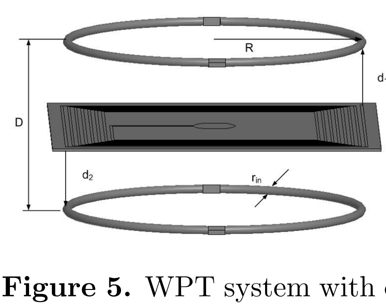

Figure 5. WPT system with one MNG metamaterial slab.

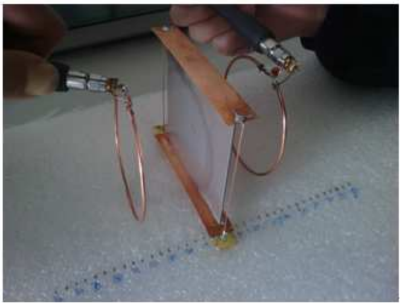

Figure 6. Photograph of the measured system with one NRI WPT system.

D the distance between the two rings, and d_1 and d_2 are the distance between the metamaterial slab and two rings, respectively. In this case, R is 35 mm, r_{in} 2 mm, and d_1, d_2 and D are variable. The NRI metamaterials were fabricated like in Section 2.

Figure 7 shows the measured results of the variation of S parameters with frequency at the distance of 80 mm when the NRI metamaterial slab is put just in the middle of the two copper rings,

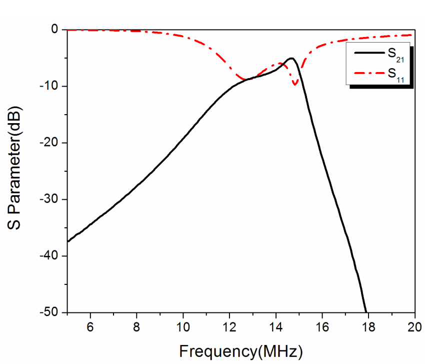

Figure 7. Characteristics of S parameters with the frequency of the WPT system with one NRI metamaterial slab when the distance of the two copper rings is 80 mm.

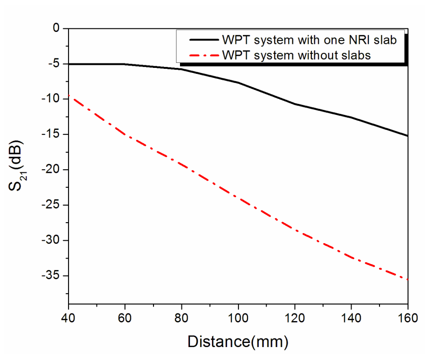

Figure 8. Comparison of measured S_{21} of the WPT system with and without NRI metamaterials when the distance varies.

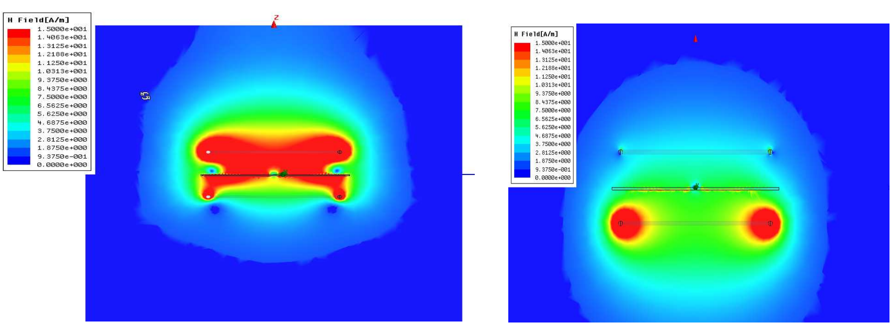

(a) (b)

Figure 9. Magnetic field of the WTP system with one NRI slab. (a) Magnetic field at the negative refractive index frequency of the NRI slab, (b) magnetic field at the non-resonant frequency of the NRI slab.

i.e., $D = 80\,\text{mm}$, $d_1 = 40\,\text{mm}$ and $d_2 = 40\,\text{mm}$. Fig. 8 shows the comparison of measured S_{21} of the proposed WPT system with and without NRI metamaterial slab when the distance varies at the frequency of 14.6 MHz. In the measurement, the copper rings were also symmetrically put and symmetrically moved. Fig. 9(a) shows the magnetic field of the new WPT system with one NRI slab at the negative refractive index frequency of the NRI slab, and Fig. 9(b) shows the magnetic field at the frequency which is not the resonant frequency of the metamaterials. So it can be seen from Fig. 7 and Fig. 9 that the new WPT system works in the mechanism of resonant coupling. And we can also find from Fig. 8 that the efficiency is considerably improved compared with the WPT system without metamaterial slabs.

Case 2. WPT System with One SMMNG Metamaterial Slab

Removing the two coated metallic strips from the NRI metamaterial slab in case 1, the property of negative refractive index changes into the property of negative permeability only. We call the modified metamaterial structures as the SMMNG (Spirals-Meander lines MNG) metamaterials in the following section, because one side pattern of the metamaterials is spirals, and the other is meandering lines. Put the SMMNG slab between the two coupling rings, and the new WPT model is the same as in Fig. 5. The comparison of measured S_{21} of the WPT system with NRI slab and with the SMMNG slab at the frequency of 14.6 MHz is given in Fig. 10 versus varied distance. So we can see from Fig. 10 that the enhancement of the WPT efficiency is almost similar and that the contribution of high transfer efficiency

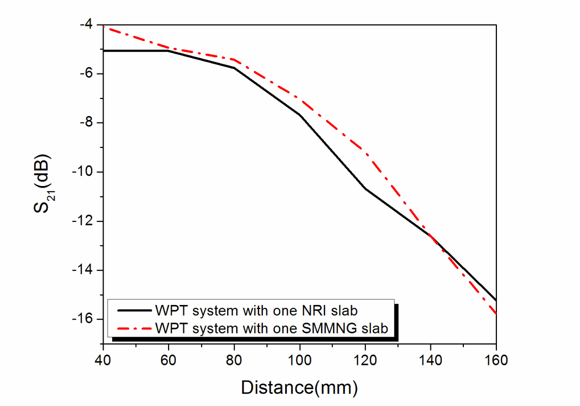

Figure 10. Comparison of measured S_{21} of the WPT system with NRI metamaterial slab and with the SMMNG metamaterial slab when the distance varies.

is due to the property of negative permeability which can make the WPT system work in the mechanism of magnetic resonance.

Case 3. WPT System with One SSMNG Metamaterial Slab

To verify the enhancement of the WPT system by using MNG metamaterials, another kind of MNG metamaterial structure firstly proposed by Chen et al. [12] is shown in Fig. 11. The metamaterials also consist of a dual-layer design by etching both sides of square spirals. According to the working frequency of the WPT system, we design and fabricate the SSMNG (Spiral-Spiral MNG) slab, as shown in Fig. 12. The two spirals are set anti-symmetrically.

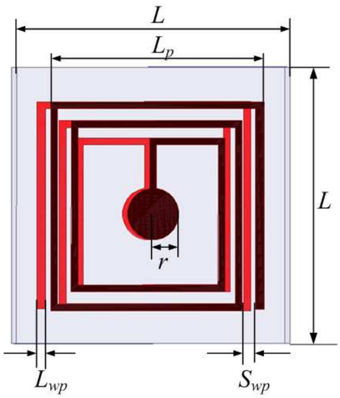

Figure 11. Solid view of the given MNG metamaterial geometry.

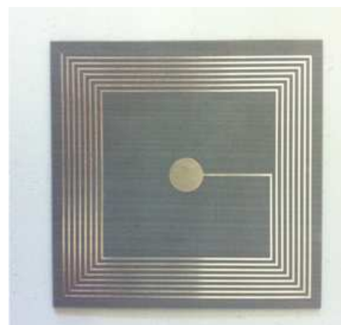

Figure 12. Top view of the fabricated given MNG metamaterial.

The effective parameters of relative permittivity ε_r, relative permeability μ_r, and refractive index n are retrieved [13] and shown in Figs. 13(a), (b) and (c), respectively. The periodicity of the proposed metamaterials is 78 mm when computing the effective material properties. It is the width of the metamaterial cell through which the electromagnetic wave passes. It can be seen that the SSMNG metamaterials do have an effective negative permeability. The parameters of the designed structure are listed in Table 2. The thickness of the substrate board is 1 mm, and the thickness of the copper foil is 0.017 mm. The surface of the copper is plated with silver. The substrate is made of dielectric material with relative permittivity of 2.6 and loss tangent of 0.015.

We apply one SSMNG slab into the WPT system, as shown in Fig. 5. Only one cell is put between the two coupling rings. The parameters of the coupling rings are the same as those of case 1. A

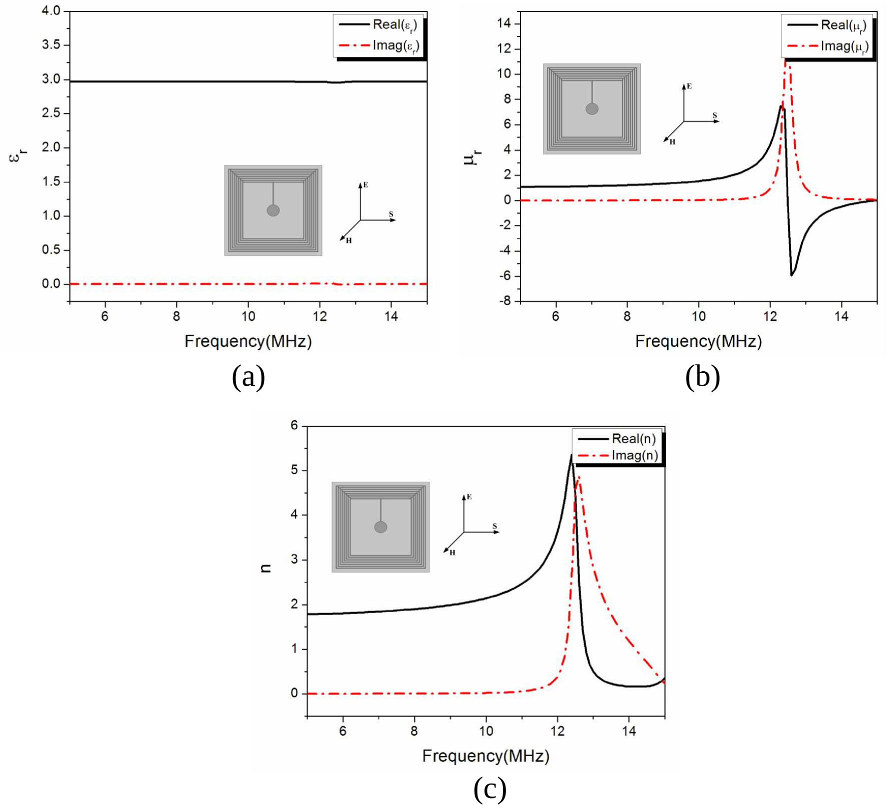

Figure 13. (a) Effective permittivity, (b) effective permeability, and (c) effective refractive index properties of the given MNG metamaterials.

photograph of the measured system is shown in Fig. 14. Fig. 15 shows the measured results of the WPT system with and without the SSMNG metamaterial slab when the two copper rings are put symmetrically at the frequency of 14.6 MHz. It can be seen that the WPT system with one SSMNG metamaterial slab can also improve the power transfer efficiency significantly, which proves that the WPT system works in the mechanism of magnetic resonance coupling after putting negative permeability metamaterials between two coupling rings.

We can see from the above three cases that the efficiency of the three cases is almost similar. So it shows that negative permeability makes contribution to the enhancement of the transfer efficiency. For simplicity, we will only use MNG metamaterial slab to improve the WPT system in the following section.

Table 2. Parameters of the SSMNG metamaterials (UNIT: mm).

L	L_p	L_{wp}	S_{wp}	r
78	70.4	0.6	1	5

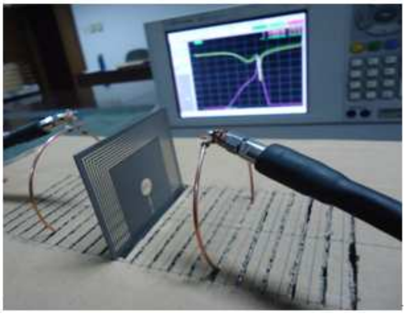

Figure 14. Photograph of the measured WPT system with one SSMNG metamaterial slab.

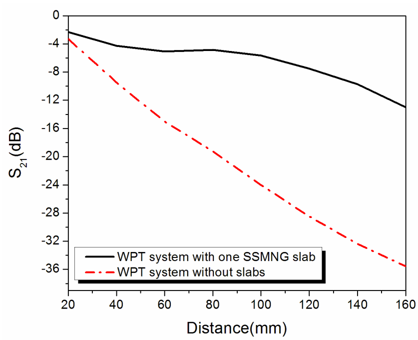

Figure 15. Comparison of the measured S_{21} of the WPT system with and without one SSMNG metamaterial slab when the distance varies.

3.2. WPT System with Two Metamaterials Slabs

The strategy is putting two metamaterial slabs between the two rings. Here, we analyze the WPT system with two SMMNG slabs for representation. This strategy is more useful in practical applications because the metamaterial slabs are easy to be integrated with the source and load devices. The parameters of the metamaterial slab, source ring and load ring are the same as those of case A. The second WPT system model is shown in Fig. 16, and a photograph of the experimental system is shown in Fig. 17. When the distance from slab to the copper ring is fixed, or $d_1 = d_2$, measured results of S_{21} of the proposed WPT system at the frequency of 14.6 MHz is shown in Fig. 18. We can see from Fig. 18 that the WPT system with two SMMNG slabs can improve the transmission efficiency significantly. We can also find that the efficiency is low when d_1 and d_2 are too small, and when d_1 and d_2 are too large the efficiency is also low. This is because the matched condition is not very good when d_1 and d_2 are small, and the coupling between the slab and the copper ring is small when d_1 and d_2 are large. And the efficiency decreases when these two cases appear. But we hope that the system can work

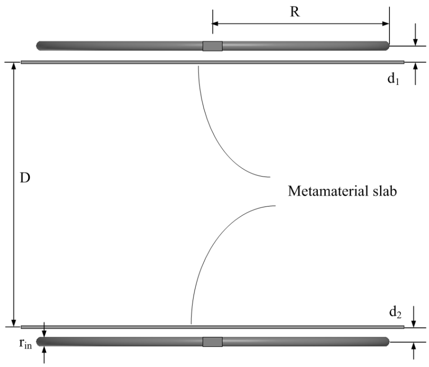

Figure 16. WPT system with two metamaterial slabs.

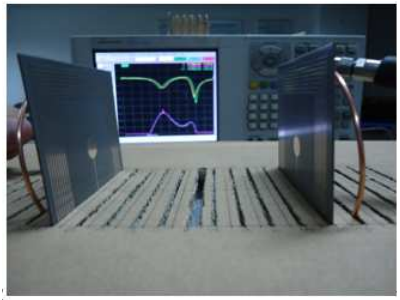

Figure 17. Photograph of the WPT system with two SMMNG slabs.

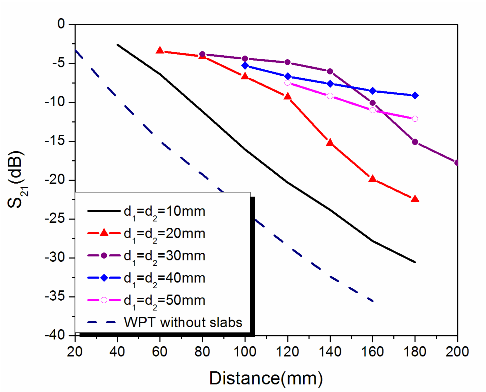

Figure 18. Measured S_{21} of the WPT system with two SMMNG slabs and that of WPT system without metamaterial slabs, and the distance between the copper ring and the slab varies from 10 mm to 50 mm.

efficiently in practical use when d_1 and d_2 are small. For this purpose we can optimize the matched network in further step to maximize the efficiency.

3.3. WPT System with Three Metamaterial Slabs

Here two SMMNG slabs and one SSMNG slab are used in the WPT system (SM-SS-SM). A photograph of the system is shown in Fig. 19. The measured results of the comparison for S_{21} of the system with and without three slabs at the frequency of 14.6 MHz are given in

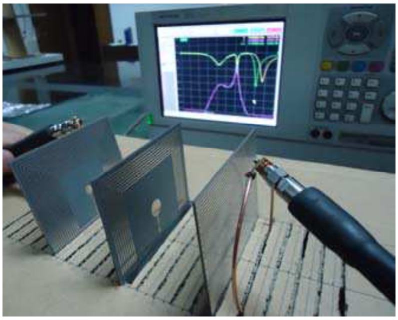

Figure 19. Photograph of the WPT system with four metamaterial slabs, one SSMNG slab and two SMMNG slabs.

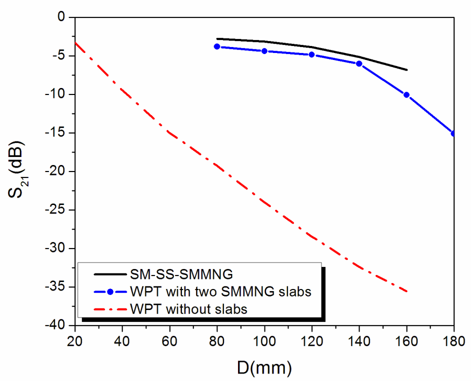

Figure 20. Comparison of measured S_{21} of the WPT system with three metamaterial slabs and the system with two slabs and without metamaterial slabs.

Fig. 20. We can see from the figure that the system with three slabs has greater efficiency than the system with two slabs and without metamaterial slabs. When the distance between the source and load rings is 140 mm, the transmission coefficient S_{21} of the WPT with three MNG slabs (SM-SS-SM) increases 27.3 dB, i.e., from −32.4 dB without slab to −5.1 dB with three MNG slabs.

3.4. WPT System with Four Metamaterials Slabs

The last case is that four metamaterial slabs are integrated by using SS-SM-SM-SS MNG slabs. A photograph of the system with four

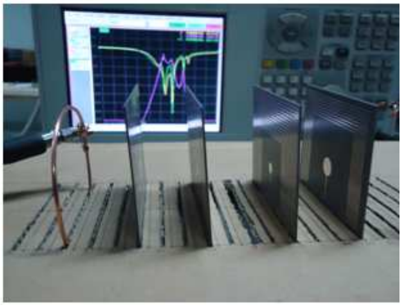

Figure 21. Photograph of the WPT system with four metamaterial slabs.

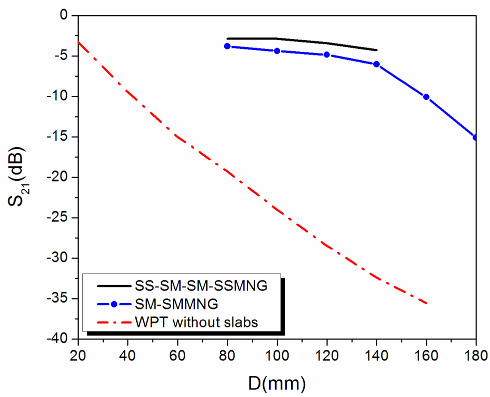

Figure 22. Measured results of the comparison for the WPT system with four metamaterial slabs with that of the system with two metamaterial slabs and without slabs.

slabs is shown in Fig. 21. The measured results of the variation of S_{21} at the frequency of 14.6 MHz with distance are shown in Fig. 22. It can be seen that the efficiency will be increased considerably, but the system with four slabs is a little complicated in this case. When the distance between the source and load rings is 140 mm, the transmission coefficient S_{21} of the WPT with four MNG slabs (SS-SM-SM-SS) increases 28.1 dB, i.e., from -32.4 dB without slab to -4.3 dB with four MNG slabs. From the above four cases, a conclusion can be made that Case B is the best scheme because the system has a good transfer efficiency with a simpler configuration.

4. CONCLUSION

In this paper, we construct a kind of high sub-wavelength negative refractive index and MNG metamaterials for wireless power transfer applications. The mechanism of the power transfer would be changed to be resonant coupling when the proposed metamaterial slabs were integrated into the WPT system, because of the negative permeability and magnetic resonant properties of the metamaterials. It can make the new WPT system resonant at the negative refractive index frequency or negative permeability frequency of the matematerials. Four implementation methods, only one MNG/NRI metamaterial slab located in the middle of two copper rings, two proposed metamaterial slabs located symmetrically between the two copper rings, three slabs located symmetrically between the two copper rings, and four slabs put between the two copper rings are considered. Experimental results verify that the WPT system integrated with metamaterials can improve the transfer efficiency significantly. When the distance between the source and load rings is 140 mm, the transmission coefficient S_{21} of the WPT with three metamaterial slabs (SM-SS-SM) increases 27.3 dB, i.e., from −32.4 dB without slab to −5.1 dB with three slabs.

ACKNOWLEDGMENT

This work is supported by the National Natural Science Foundation of China under Grant No. 61072017 and supported partly by the Program for New Century Excellent Talents in University of China, the Natural Science Basic Research Plan in Shaanxi Province of China (No. 2013JZ019), the National Key Laboratory Foundation, and the Fundamental Research Funds for the Central Universities (K5051202051, K5051302025).

REFERENCES

1. Tesla, N., "The transmission of electrical energy without wires as a means for furthering peace," *Electrical World and Engineer*, 21—24, January 7, 1905.
2. Kurs, A., A. Karalis, R. Moffatt, J. D. Joannopoulos, P. Fisher, and M. Soljačić, "Wireless power transfer via strongly coupled magnetic resonance," *Science*, Vol. 317, 83–86, Jul. 6, 2007.
3. Huang, D., Y. Urzhumov, D. R. Smith, K. H. Teo, and J. Zhang, "Magnetic superlens-enhanced inductive coupling for wireless

power transfer," *Journal of Applied Physics*, Vol. 111, 064902, 2012.

4. Cannon, B. L., J. F. Hoburg, D. D. Stancil, and S. C. Goldestein, "Magnetic resonant coupling as a potential means for wireless power transfer to multiple small receivers," *IEEE Transactions on Power Electronics*, Vol. 24, No. 7, 1819–1825, Jul. 2009.
5. Choi, J. and C. Seo, "High-efficiency wireless energy transmission using magnetic resonance based on metamaterial with relative permeability equal to -1," *Progress In Electromagnetics Research*, Vol. 106, 33–47, 2010.
6. Wang, B., K. H. Teo, T. Nishino, W. Yerazunis, J. Barnwell, and J. Zhang, "Experiments on wireless power transfer with metamaterials," *Appl. Phys. Lett.*, Vol. 98, 254101, 2011.
7. Urzhumov, Y. and D. R. Smith, "Metamaterial-enhanced coupling between magnetic dipoles for efficient wireless power transfer," *Phys. Rev. B*, Vol. 83, 205114, 2011.
8. Li, L., Y. C. Fan, S. X. Yu, C. Zhu, and C. H. Liang, "Design, fabrication and measurement of highly sub-wavelength double negative metamaterials at HF frequencies," *Journal of Applied Physics*, Vol. 113, 213712, 2013.
9. Pendry, J. B., "Extremely low frequency plasmons in metallic microstructures," *Phys. Rev. Lett.*, Vol. 76, 4773–4776, 1996.
10. Shelby, R. A., D. R. Smith, and S. Schultz, "Experimental verification of a negative index of refraction," *Science*, Vol. 292, 77–79, 2001.
11. Smith, D. R., W. J. Padilla, and D. C. Vier, "Composite medium with simultaneously negative permeability and permittivity," *Phys. Rev. Lett.*, Vol. 84, No. 18, 4184–4187, 2000.
12. Chen, W. C., C. M. Bingham, K. M. Mak, N. W. Caira, and W. J. Padilla, "Extremly sub-wavelength planar magnetic metamaterials," *Phys. Rev. B*, Vol. 85, 201104, 2012.
13. Smith, D. R., D. C. Vier, Th. Koschny, and C. M. Soukoulis, "Electromagnetic parameter retrieval from inhomogeneous metamaterials," *Phys. Rev. E*, Vol. 71, 036617, 2005.